LANGMUIR

Article

pubs.acs.org/Langmuir

Interaction between Polymeric Additives and Secondary Fluids in Capillary Suspensions

Boris Bitsch,*[,†] Björn Braunschweig,[‡] and Norbert Willenbacher[†]

[†]Institute of Mechanical Engineering and Mechanics, Karlsruhe Institute of Technology (KIT), Gotthard-Franz-Strasse 3, 76131 Karlsruhe, Germany

[‡]Institute of Particle Technology (LFG), Friedrich-Alexander University Erlangen-Nürnberg (FAU), Cauerstrasse 4, 91058 Erlangen, Germany

ABSTRACT: Capillary suspensions are ternary systems including a solid and two liquid phases representing a novel formulation platform for pastes with unique processing and end-use properties. Here we have investigated aqueous suspensions of non-Brownian graphite particles including different polymers commonly used as thickening agents or binders in paste formulations. We have studied the interaction between these additives and organic solvents in order to elucidate its effect on the characteristic formation of a particle network structure in corresponding ternary capillary suspension systems. Organic solvents with different polarity have been employed, and in the presence of nonadsorbing poly(ethylene oxide), all of them, whether they preferentially wet the graphite surface or not, induce the formation of a network structure within the suspension as indicated by a strong change in rheological properties. However, when the adsorbing polymers carboxymethylcellulose and poly(vinylpyrrolidone) are included, the drastic change in rheological behavior occurs only when polar organic solvents are used as secondary liquids. Obviously, these solvents can form pendular bridges, finally resulting in a sample-spanning particle network. Vibrational sum frequency spectroscopy provides evidence that these polar liquids remove the adsorbed polymer from the graphite particles. In contrast, nonpolar and nonwetting solvents do not force polymer desorption. In these cases, the formation of a percolating network structure within the suspensions is presumably prevented by the strong steric repulsion among graphite particles, not allowing for the formation of particle clusters encapsulating the secondary liquid. Accordingly, polymeric additives and secondary fluids have to be carefully selected in capillary suspension formulations, then offering a new pathway to customize paste formulations. The polymer may serve to adjust an appropriate viscosity level, and the capillary bridging induces the desired degree of shear thinning. Alternatively, the polymer may be selected with respect to its binding properties in the final dry product, and capillary bridging may be used to control the flow and processing behavior of the wet paste.

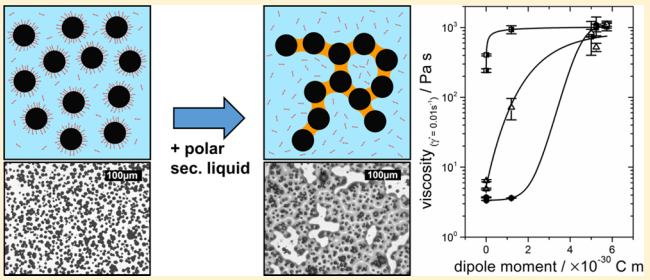

1. INTRODUCTION

Suspensions are ubiquitous in nature, industrial processes, and everyday life. Blood is circulating in our bodies, ceramics and other inorganic matter are processed as finely dispersed in a liquid continuous phase, and coatings and adhesives are applied as suspensions. Food, personal care, crop protection, and pharmaceutical products are utilized in suspended form.[1,2]

Dispersibility, stability against aggregation and sedimentation, and flow behavior are crucial features during the production, storage, and application of such fluids. Therefore, technical or commercial products generally include additives such as surfactants, dispersing agents, thickeners, or binders to guarantee the desired processing or end-use properties, and the interactions among these ingredients are often decisive with respect to the behavior of the complex formulations.[3,4]

Recently, a new type of suspension, so-called capillary suspensions first described by Koos and Willenbacher,[5] have attracted a great amount of attention.[6,7] These ternary systems include fine solid particles suspended in a primary or bulk fluid phase as well as a small fraction of a secondary liquid immiscible with the bulk fluid. Strong attractive capillary forces among the suspended particles induced by the addition of the secondary fluid result in the formation of a sample-spanning network, regardless of whether this liquid wets the particles better or worse than the bulk phase.

Two types of capillary suspensions are distinguished depending on the three-phase wetting angle Θ_{3p} that the secondary liquid forms against the solid surface in the bulk-phase environment. In the pendular state ($\Theta_{3p} < 90°$), the secondary liquid wets the solid phase better than the continuous phase and forms pendular bridges between the particles. In the case where $\Theta_{3p} > 90°$, termed the capillary state, the particles form clusters around small volumes of the second fluid.[8] Both scenarios finally result in a percolating

Received: October 18, 2015
Revised: January 25, 2016
Published: January 25, 2016

DOI: 10.1021/acs.langmuir.5b03861
Langmuir 2016, 32, 1440−1449

particle network which gives rise to a pastelike suspension texture and strongly shear-thinning flow behavior. Capillary suspensions are highly resistant to sedimentation, and their flow properties can be tuned over a wide range to meet different processing or application demands. A broad range of innovative materials including novel food formulations, such as heat-stable and low-calorie chocolate spreads,[9] capillary-suspension-based foams,[10,11] pastes for printed electronics (e.g., lithium ion battery electrodes or front-side metallization of solar cells with unique shape accuracy and surface uniformity[12]), and precursors for highly porous ceramic and glass membranes have been developed.[13,14] The capillary suspension concept has also been used to control structure formation in particle-laden polymer blends[15] and to assemble metals and nanoparticles into novel nanocomposite superstructures.[16]

In the next step of a rational material design, the effect of further additives frequently used in suspension-based products has to be explored rigorously. Recently, it has been shown that the addition of a surfactant (either to the bulk or to the secondary fluid) strongly affects structure formation and can lead to a drastic reduction in yield stress and viscosity. This reduction was found to be much more pronounced than expected from the observed decrease in interfacial tension and could be attributed to an increase in the contact angle as well as a partial trapping of the secondary fluid within surfactant micelles.[17]

In the present study, we discuss the influence of polymeric additives frequently used as thickeners or binding agents on the formation of capillary suspensions. An aqueous suspension of non-Brownian graphite particles was utilized as a model system for these investigations. Because of the size of the particles and the viscosity of the solvent, Brownian motion is not relevant on the experimental time scale that is relevant here. Graphite and carbon materials are widely used in aqueous or nonaqueous formulations, in particular, for energy storage and energy conversion applications.[18−22] Carboxymethylcellulose (CMC), poly(vinylpyrrolidone) (PVP), and poly(ethylene oxide) (PEO) were chosen as water-soluble polymers with different affinity for graphite surfaces. Finally, organic solvents with varying polarity were investigated as secondary fluids. All of these secondary liquids are immiscible with water and can potentially form capillary suspensions in either the pendular or capillary state.

For each system, we investigated rheological and interfacial properties (i.e., shear viscosity η, storage and loss modulus G' and G'', interfacial tension Γ, and three-phase wetting angle Θ_{3p}). Furthermore, we examined the adsorption and desorption of polymer molecules on graphite surfaces and the interaction between these additives and secondary fluids via spectroscopic methods. The investigated aqueous graphite systems form capillary suspensions irrespective of the polarity and the wetting angle of the organic secondary fluid when no adsorbing polymer is present. When adsorbing polymers are included, spectroscopic results reveal that only polar solvents are able to displace these polymers from the particle surface. These polar secondary fluids with wetting angles smaller than 90° form pendular bridges and a percolating particle network even when adsorbing polymers are used in the formulation. In contrast, nonpolar secondary fluids with wetting angles larger than 90° are not able to remove the polymers from the particles and do not form capillary suspensions. The insights gained in this study represent a major step toward a better understanding of interactions in complex, technically relevant formulations based on capillary suspensions.

2. EXPERIMENTAL SECTION

2.1. Suspension Preparation. Commercial-grade polymers CMC, PVP, and PEO were used in this study. CMC with an average molecular weight M_w of between 1 400 000 and 1 500 000 g/mol and a degree of substitution of ≥0.8 was purchased from Daicel (CMC 2200, Daicel Corporation, Osaka, Japan). PVP K90 (M_w = 360 000 g/mol) was received from Carl Roth GmbH (Karlsruhe, Germany). Moreover, poly(ethylene oxide) from Sigma-Aldrich (Buchs, Switzerland) with M_w = 1 000 000 g/mol was utilized. Furthermore, pure glycerol, purchased from Carl Roth, with a density of 1.26 g/cm^3 and a viscosity of η = 1.4 Pa s at 20 °C was utilized. The synthetic graphite powder used here is commercially available from China Steel Chemical Corporation (SMGP-A, Kaohsiung, Taiwan) and contains isometric particles with a volume-based average diameter of $d_{50,3}$ = 7.8 μm, a narrow size distribution, and a density of 2.2 g/cm^3. A SEM picture of the utilized graphite powder is shown in Figure 1. Graphite typically

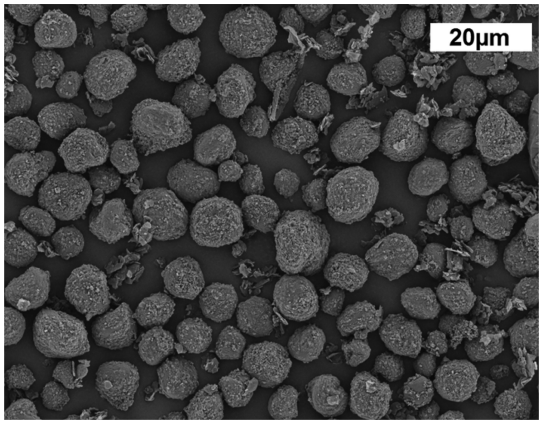

Figure 1. SEM image of the utilized, commercially available graphite powder.

exhibits surface energy values of about 40 to 50 mN/m.[23,24] The following secondary liquids from Carl Roth GmbH or Merck Millipore Corporation (Darmstadt, Germany) were used: *n*-dodecane (>99%), *n*-heptane (>99%), toluene (>99.5%), 1-octanol (>99%), octanoic acid (>99%), and heptanoic acid (>99%). All secondary liquids are immiscible with water and glycerol.

CMC and PVP were dissolved in water using a propeller stirrer (diameter 55 mm, 800 rpm for 3 h). PEO was dissolved using a vibrating plate for 144 h. All solutions were optically transparent after the described dissolution procedure was performed. The amount of polymer was chosen to adjust the zero shear viscosity of the solution to about 1.4 Pa s (CMC, 0.7 vol %; PVP, 13.6 vol %; PEO, 2.7 vol %). Regarding the polymer concentration, all aqueous solutions are in the transition zone between the semidilute and concentrated regime.[25,26]

Subsequently, graphite particles (20 vol %) were added to the solutions using a dissolver mixer (RZR 2021, Heidolph Instruments, Schwabach, Germany, dissolver blade, diameter 50 mm, mixing at 1300 rpm for 15 min). Finally, 2 vol % of a secondary fluid was added to the suspension while dissolver stirring was applied at 1000 rpm for 10 min.

2.2. Interfacial Properties. Pendant and sessile drop methods were applied to determine interfacial properties of the investigated material systems. For interfacial tension measurements, a drop of polymer solution was dispensed using a hollow needle (inner diameter d_i = 400 μm) in a glass cuvette filled with the appropriate secondary fluid. Drop-shape images taken with a camera system (AVT Stingray F-033B, Allied Vision Technology: 1/2″ CCD, 656 × 492 square pixels) were analyzed, and interfacial tension values were calculated using commercially available software (drop shape analysis, Krüss

DOI: 10.1021/acs.langmuir.5b03861
Langmuir 2016, 32, 1440−1449

Table 1. Interfacial Tension between Bulk Solutions and Secondary Liquids as determined by the Pendant Drop Method[a]

bulk solution: / sec. fluid	H_2O, mN m^{-1}	CMC−H_2O, mN m^{-1}	PVP−H_2O, mN m^{-1}	PEO−H_2O, mN m^{-1}	glycerol, mN m^{-1}	dipole moment × 10^{-30} C m[30,31]
1-octanol	8.0	7.8	5.9	6.8	4.4	5.7
octanoic acid	7.8	6.8	1.6	3.9	3.7	5.2
heptanoic acid	6.4	5.6	1.9	3.1	2.3	5.0
n-dodecane	50.4	43.5	28.7	29.1	28.3	0.0
n-heptane	49.6	45.1	28.3	28.3	27.3	0.0
toluene	36.0	33.8	17.3	17.1	19.3	1.2

[a]The experimental error is <3% for all measured values.

GmbH, Hamburg, Germany). For three-phase wetting angle measurements, a low-porosity graphite plate (porosity ≤10%, from Graphite Cova GmbH, Röthenbach, Germany) was immersed in the polymer solution and a secondary fluid drop was dispensed on the plate surface. Three-phase wetting angles of the sessile drops were evaluated by applying the tangent method.

2.3. Rheological Investigations. A RheoStress 1 (Thermo Scientific, Karlsruhe, Germany) rotational rheometer equipped with a plate−plate measuring cell (d_{PP} = 35 mm, gap width h_{PP} = 1 mm) and a cone−plate measuring cell (d_{CP} = 60 mm, cone angle Θ_{cone} = 1°), respectively, were used to perform shear-stress-controlled steady and oscillatory shear measurements. The cone−plate system was used for the pure polymer solutions, and the plate−plate system was used for the graphite suspensions. Logarithmic shear stress ramps (initial stress 0.1 or 1.0 Pa, final stress 100 or 1000 Pa, 300 s measurement time) were applied in steady-shear experiments. Small-amplitude oscillatory shear experiments covering a frequency range from 0.1 to 100 rad s^{-1} were performed at a constant shear stress of between 0.8 and 3 Pa. Strain-sweep experiments performed prior to the frequency sweeps confirmed that the chosen shear stress was sufficiently low to provide a linear material response at all investigated frequencies. A solvent trap was used to avoid the evaporation of the volatile components of the suspensions during the experiments.

2.4. Sum-Frequency Generation (SFG). Vibrational SFG spectra were recorded with frequency tunable ∼80 fs IR pulses of >200 cm^{-1} full width at half-maximum (fwhm) bandwidth and with etalon-filtered femtosecond pulses at 800 nm wavelength, with <6 cm^{-1} bandwidth and ∼1.6 ps pulse durations after etalon filtering. The IR and the 800 nm beams were overlapped in space and time at the interface. The reflected sum-frequency (SF) photons were collected and detected with a combination of a spectrograph (Andor, Shamrock 303i) and an intensified CCD camera (Andor, iStar). The acquisition time per IR wavelength was 60 s, while the polarizations of sum-frequency, 800 nm, and IR beams were fixed to s, s, and p (ssp), respectively. The typical focal sizes from which the SF photons can be collected were 200 μm parallel to the plane of incidence and 100 μm perpendicular to it. In principle, this also determines the minimum sample size that can be chosen without having to focus the laser beams more tightly. Samples ideally have to be planar for our experimental conditions.

SFG intensities can be expressed as a function of resonant and nonresonant excitations of molecules at the interface, and the SFG signal is resonantly enhanced when the frequency of the IR beam is close to the frequency of vibrational modes from interfacial molecules.[27,28]

$$I(\omega_{SF}) \propto \left| \chi^{(2)}_{NR} + \sum_q \frac{A_q}{\omega_q - \omega + i\Gamma_q} \right|^2 I_{IR} I_{vis}$$

Here, $A_q = N \int f(\Omega)\, \beta_q(\Omega)\, d(\Omega)$ is the oscillator strength of an SFG active vibrational mode, which is a function of the molecular number density N as well as the molecular orientation distribution $f(\Omega)$ and the molecular hyperpolarizability β_q. Since SF photons are coherently generated, the average over all molecular orientations which are realized inside a sample needs to be considered. Because only a preferential alignment (e.g., that due to the presence of an interface) gives rise to nonzero amplitudes A_q, vibrational SFG is inherently interface-selective for materials that have inversion symmetry. For this reason, molecules in the bulk (e.g., within a thicker film at distances ≫1 nm away from the interfacial plane or in a bulk fluid) are ignored due to symmetry reasons. As a consequence, vibrational SFG provides information on the chemical identity of adsorbed species as well as their orientation and concentration. However, when the latter change simultaneously, it is difficult to obtain quantitative information on molecular order and the surface excess.[29]

2.5. Sample Preparation for SFG Spectroscopy. Because of the extremely high optical density of the capillary suspensions, it was not possible to perform in situ SFG spectroscopy. For that reason, we have studied layers of particles that were prepared directly from the suspensions with preadsorbed CMC and PVP adlayers. These layers are used as a model system for the particles within the suspensions under investigation, and we assume that during particle deposition, predominant interfacial properties and adsorbed surface species are preserved. In fact, this assumption is corroborated by our results shown in the Results section. Particle layers from suspensions as discussed above were deposited on air-plasma-treated microscope slides (Carl Roth) and were investigated with SFG after being dried in a stream of N_2. Optical microscopy images of the particle layers were taken in order to ensure similar particle coverage of the substrate. Subsequent to particle deposition and imaging, SFG spectra were recorded prior to and after washing with the organic solvents used as secondary fluids here in order to examine whether these polymers are removed from the particle surface. For that purpose, graphite particle layers were covered with the secondary liquid, and the excess liquid was subsequently partially removed in a stream of nitrogen gas. This procedure yielded optically smooth films. We point out that the thickness of the film does not impact our interfacial selectivity because molecules not attached to the graphite surface do not contribute to the SFG spectra.

3. RESULTS AND DISCUSSION

3.1. Interfacial Tension and Three-Phase Wetting Angle of the Investigated Bulk and Secondary Fluids. Interfacial tension between the organic solvents used as secondary fluids and the aqueous polymer solutions used as bulk fluids was determined with the pendant drop method. The results are summarized in Table 1, which also includes the dipole moments of the organic liquids taken from the literature.[30,31] Data for pure water and glycerol are included for reference. Polar organic liquids with a high dipole moment show low interfacial tension values against the investigated bulk fluids. Nonpolar secondary fluids, in contrast, exhibit high interfacial tension values. The addition of CMC to water only slightly reduces the interfacial tension as expected since the high-molecular-weight CMC molecules are not surface-active. In contrast, PVP and PEO lower the interfacial tension against all organic fluids. We propose that this might presumably be due to the polydispersity of these polymeric additives. Traces of short-chained, surface-active molecules that are present in the

DOI: 10.1021/acs.langmuir.5b03861
Langmuir 2016, 32, 1440−1449

polymer solution may cause the observed reduction in interfacial tension. The presence of traces of low-molecular-weight, surface-active molecules is particularly more likely for the PEO and especially the PVP solution due to the high polymer concentration in these systems compared to that in the CMC solutions.

Three-phase wetting angle Θ_{3p} data for secondary fluids surrounded by polymer solution or by pure water on graphite as determined utilizing the sessile drop method are displayed in Figure 2 as a function of the secondary fluid dipole moment.

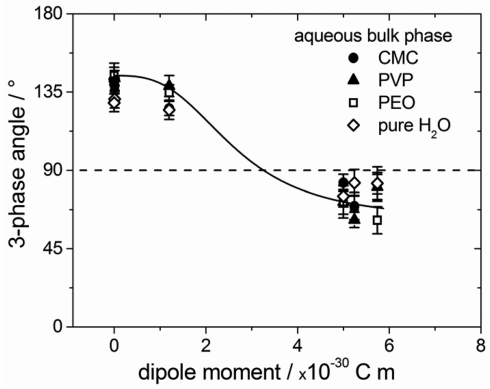

Figure 2. Three-phase wetting angle of different secondary liquids on a low-porosity graphite plate while surrounded by pure water or aqueous solutions of CMC, PVP, and PEO, respectively. Data were determined by applying the sessile drop method. The solid line serves to guide the eye.

Polar fluids exhibit wetting angles of $\Theta_{3p} < 90°$, whereas nonpolar solvents form wetting angles of $\Theta_{3p} > 90°$. Irrespective of the type of polymer dissolved in the aqueous phase, the three-phase wetting angle Θ_{3p} remains either <90° or >90° mostly depending on the polarity of the utilized organic liquid. The potential adsorption of polymer chains on the graphite surface as reported for PVP and CMC[32−34] obviously does not affect the wetting behavior of a macroscopic droplet of organic liquid to such an extent that it could be resolved with our sessile drop technique. In accordance with the concept of capillary suspensions,[5] we expect that polar secondary fluids form capillary suspensions in the pendular state, whereas nonpolar secondary fluids lead to capillary suspensions in the capillary state when added to aqueous graphite suspensions.

3.2. Flow Properties of Polymer Solutions and Corresponding Graphite Suspensions. To eliminate the influence of the continuous-phase viscosity on the formation of a capillary network during the emulsification of the secondary fluid, the zero shear viscosity of the investigated polymer solutions was adjusted to a value of about 1.4 Pa s by adding appropriate fractions of each polymer. Additionally, glycerol was used as a pure Newtonian bulk fluid (η = 1.4 Pa s). Figure 3 compares the flow curves of pure polymer solutions and glycerol to the corresponding suspensions including 20 vol % graphite. As evident from Figure 3a, the investigated CMC and PEO solutions exhibit a high degree of shear-thinning, whereas the PVP solution is only slightly shear-thinning and glycerol shows ideal Newtonian behavior.

The increase in viscosity due to the added graphite particles is shown in Figure 3b in terms of relative viscosity $\eta_{rel} = \frac{\eta_{suspension}}{\eta_{solvent}}$ as a function of shear rate. For the suspensions based on CMC

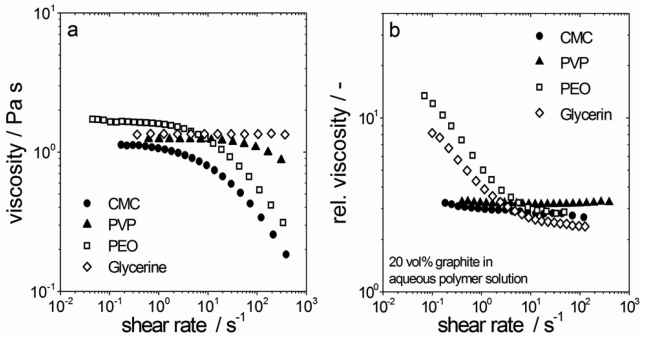

Figure 3. (a) Viscosity vs shear rate data for glycerol and aqueous polymer solutions based on CMC (0.7 vol %), PVP (13.6 vol %), and PEO (2.7 vol %). (b) Relative viscosity $\left(\eta_{rel} = \frac{\eta_{suspension}}{\eta_{solvent}}\right)$ as a function of shear rate for suspensions of 20 vol % graphite particles in different polymer solutions (polymer concentrations equal to those in part a) and glycerol. All error bars are as large as the sizes of the different symbols.

and PVP solutions, η_{rel} = 3.5 irrespective of the applied shear rate, indicating that graphite particles are well dispersed in these stable suspensions. This is attributed to a steric stabilization provided by the polymer that is partially adsorbed to the particle surface.[32−34] The absolute value of η_{rel} is about twice as high as for suspensions of ideal hard spheres,[35,36] and this is attributed to deviations from the ideal spherical shape of the utilized graphite (Figure 1).

In contrast, the suspensions based on PEO solutions and glycerol as continuous phases exhibit a monotonic increase in η_{rel} with deceasing shear rate reaching absolute values of between 8 and 15 in the low-shear regime. This is attributed to particle aggregation and network formation due to strong van der Waals attraction among particles. At high shear rates, η_{rel} approaches a similar level as observed for the suspensions including CMC and PVP, indicating that the aggregates break in strong flow.

3.3. Flow Properties of Graphite Suspensions with Secondary Liquids. The formation of a sample-spanning capillary network within a suspension upon addition of a secondary fluid, immiscible with the bulk fluid, is generally accompanied by a drastic increase in low-shear viscosity. An increase by about one order of magnitude in the low-shear viscosity is a reasonable indicator of the successful creation of a capillary network. Furthermore, capillary suspensions show gel-like flow properties (i.e., high and almost frequency-independent shear modulus values[5]). The flow properties of graphite suspensions with different secondary liquids were characterized via steady and oscillatory shear rheometry. In Figure 4a, flow curves of aqueous CMC−graphite suspensions with different secondary liquids are shown. Obviously, the addition of heptane, dodecane, and toluene has no effect on the shear rheology of the basic suspension. However, adding 2 vol % octanol, octanoic acid, or heptanoic acid results in a drastic increase in the low-shear viscosity of more than two decades and strong shear thinning. Similar results are obtained for aqueous PVP−graphite suspensions (Figure 4b). The polar secondary fluids lead to an increase in low-shear viscosity, whereas heptane and dodecane do not change the flow curves significantly. Among the nonpolar solvents, only toluene leads to a substantial increase in low-shear viscosity. However, this increase is much less pronounced than in the case of the highly

DOI: 10.1021/acs.langmuir.5b03861
Langmuir 2016, 32, 1440−1449

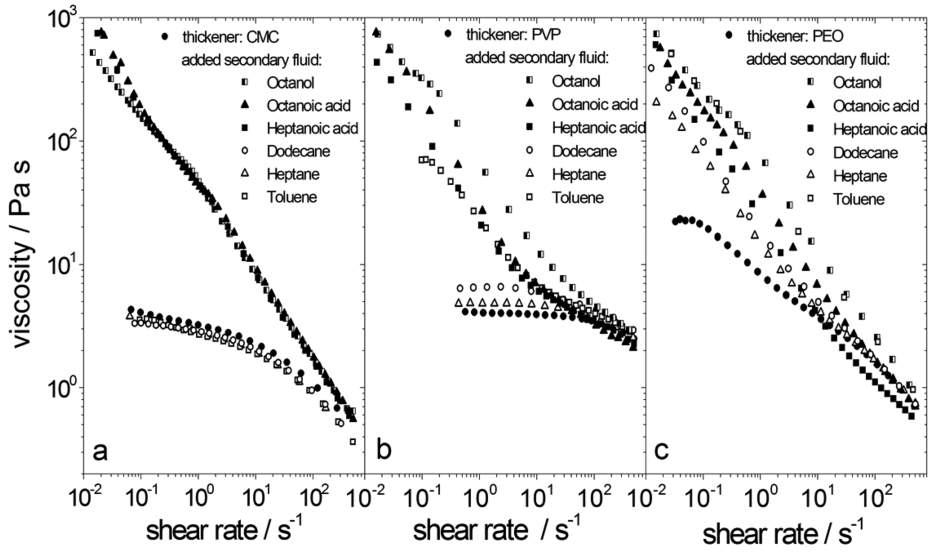

Figure 4. Viscosity curves as a function of shear rate for aqueous graphite suspensions including (a) CMC, (b) PVP, and (c) PEO. Different organic liquids (2 vol %) were added to the basic suspension. Error bars are not larger than the sizes of the different symbols.

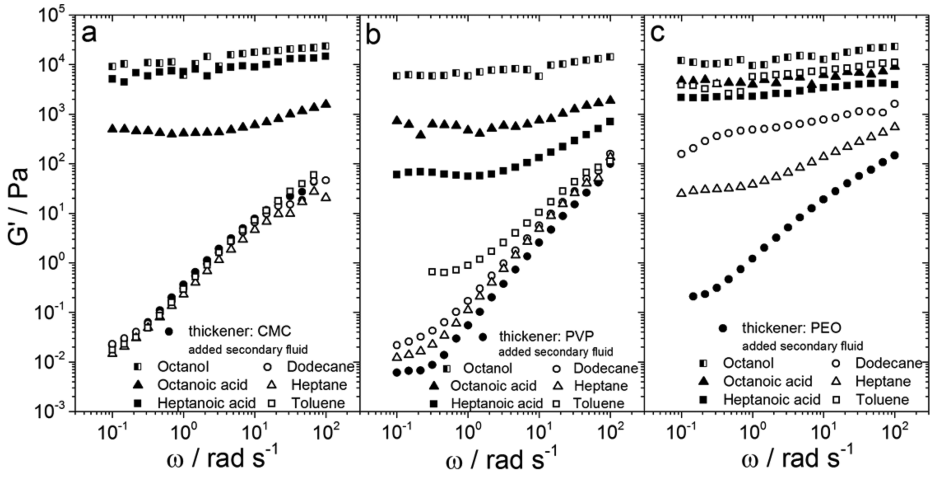

Figure 5. Storage modulus G' as a function of angular frequency ω for aqueous graphite suspensions including (a) CMC, (b) PVP, and (c) PEO. Different organic liquids (2 vol %) were added to the basic suspension. Error bars are not larger than the sizes of the different symbols.

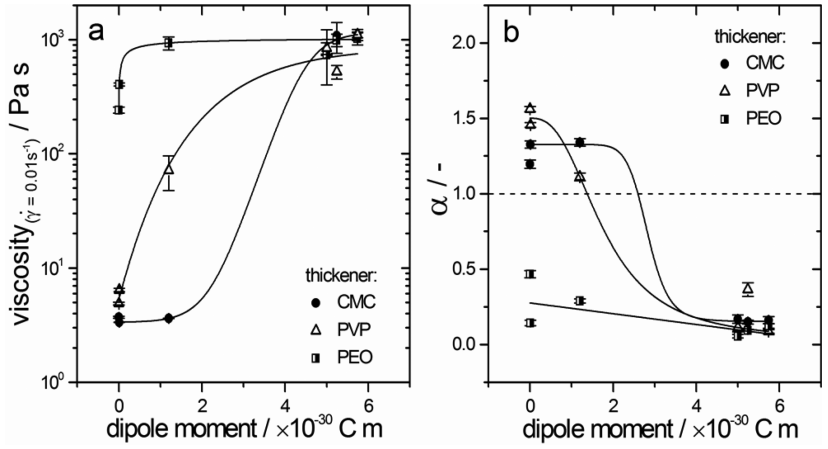

Figure 6. (a) Low-shear viscosity determined at $\dot{\gamma}$ = 0.01 s^{-1} and (b) power law exponent α vs secondary liquid dipole moment of the added secondary liquid for ternary suspensions including different polymers. Data for exponent α were derived from power law fits ($G'(\omega) \propto \omega^{\alpha}$) to experimental storage modulus data shown in Figure 5. The solid lines serve to guide the eye.

DOI: 10.1021/acs.langmuir.5b03861
Langmuir 2016, 32, 1440−1449

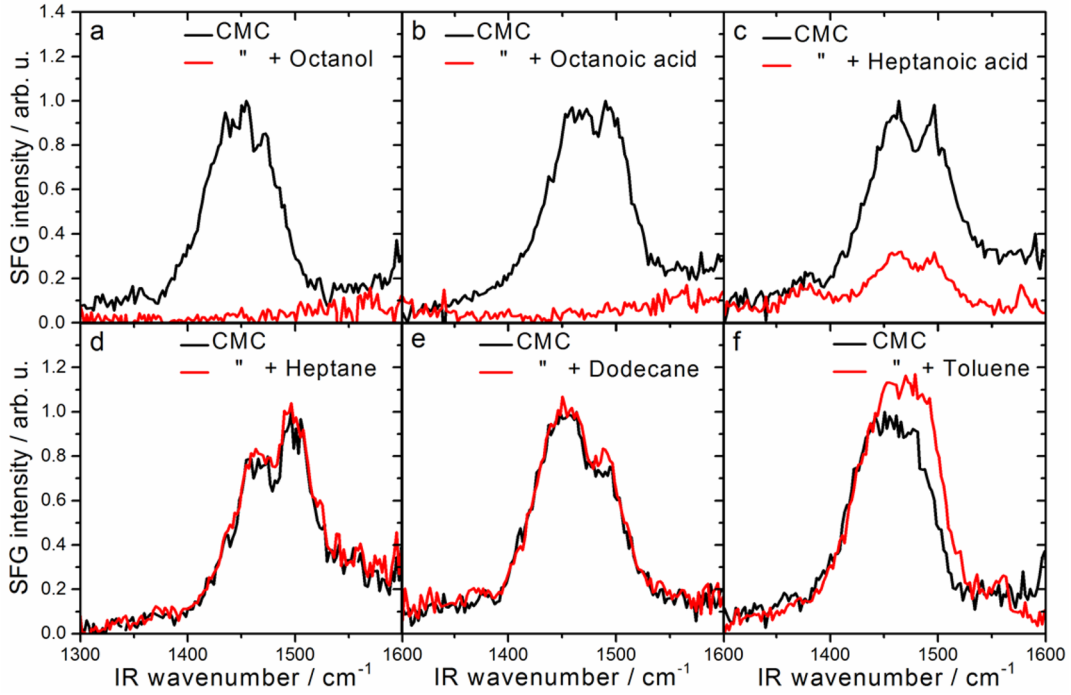

Figure 7. Vibrational SFG spectra obtained at the interfaces of graphite particles which were suspended in aqueous CMC solution before (black lines) and after (red lines) wetting with secondary fluids: (a) octanol, (b) octanoic acid, (c) heptanoic acid, (d) heptane, (e) dodecane, and (f) toluene.

polar solvents. A different response to the addition of a secondary fluid is observed when PEO is included in the aqueous graphite suspension. As shown in Figure 4c, an increase in low-shear viscosity of almost two orders of magnitude is achieved for all added secondary liquids. Only the addition of heptane results in a slightly lower viscosity increase at low shear rates. In summary, the creation of a capillary suspension seems to be successful with all added secondary fluids when PEO is utilized as a polymeric additive, whereas this self-assembling structure formation takes place only with polar solvents octanol, octanoic acid, and heptanoic acid when CMC or PVP is present as polymeric additive.

These findings are corroborated by the shear modulus data shown in Figure 5. Figure 5a,b displays G' values as a function of angular frequency ω for graphite suspended in aqueous CMC and PVP solutions with different organic liquids added as secondary fluid. For both polymers, the added polar secondary liquids octanol, octanoic acid, and heptanoic acid lead to a drastic increase in G' at low frequencies, resulting in an essentially frequency-independent G' regime covering three decades in ω. For heptane, dodecane, and toluene, no significant change in G' could be observed compared to the basic suspension. However, when PEO was used as polymeric additive all secondary liquids lead to a high, frequency-independent level of G' (Figure 5c) characteristic of particulate gels and networks.

Similar shear and oscillatory rheological experiments have been performed with pure glycerol as the bulk phase (not shown here). After the addition of each secondary liquid, a drastic increase in low-shear viscosity and a frequency-independent modulus G' were observed.

A high, frequency-independent shear modulus and a high viscosity at low shear rates are characteristic features of gel-like suspensions with a network structure induced by strong attractive interactions among particles. For the ternary solid/fluid/fluid systems investigated here, a strong increase in low-shear viscosity and the emergence of a frequency-independent modulus $G'(\omega)$ upon addition of the secondary fluid clearly indicate the successful formation of a capillary suspension. Accordingly, these quantities are displayed in Figure 6 as a function of the secondary fluids' dipole moment. Figure 6a shows the viscosity of the ternary suspensions obtained at a shear rate of $\dot{\gamma} = 0.01\ s^{-1}$. The frequency dependence of the storage moduli is characterized by exponent α deduced from a fit of the power law $G'(\omega) \propto \omega^{\alpha}$ to the experimental data shown in Figure 5, and the α values derived for different polymer−secondary liquid combinations are displayed in Figure 6b. Secondary fluids with a high dipole moment generally result in suspensions with low α values close to zero ($0 < \alpha < 0.5$) and high low-shear viscosities. For the nonpolar secondary fluids, high low-shear viscosities and low α values are found when PEO is present. However, the increase in low-shear viscosity is weak and the frequency dependence of G' is pronounced when PVP or CMC is added. From these results, we conclude that the formation of a capillary network strongly depends on the type of polymer present in the aqueous phase when nonpolar secondary fluids are added. Capillary suspensions made with polar secondary fluids exhibit very similar absolute values of the low-shear viscosity independent of the included polymer. In this case, network formation is not affected by the presence of the polymer molecules even if they partially adsorb on the particle surface in the pure, two-component suspensions.

3.4. Displacement of Adsorbed Polymers from Graphite Particles. As discussed above, both CMC and PVP are likely to adsorb on graphite surfaces.[32−34] When these polymers are present in the graphite suspensions, only polar secondary fluids with wetting angles of <90° form stable capillary suspensions. On the other hand, there is no indication that PEO adsorbs on the graphite surface. This polymer is

DOI: 10.1021/acs.langmuir.5b03861
Langmuir 2016, 32, 1440−1449

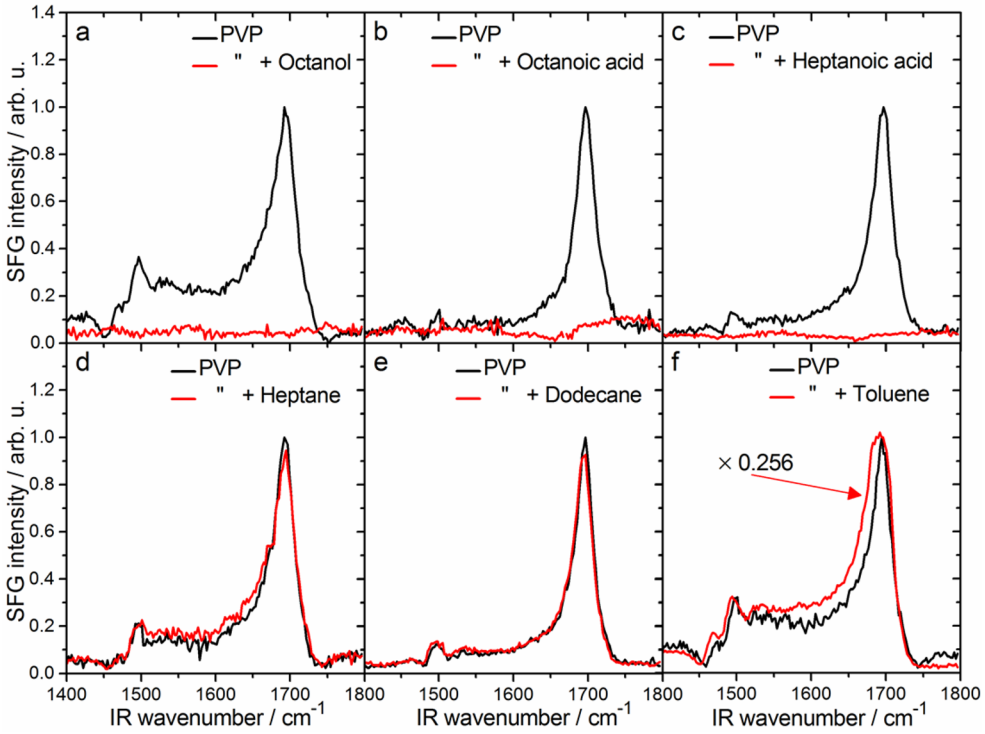

Figure 8. Vibrational SFG spectra obtained at the interfaces of graphite particles which were suspended in aqueous PVP solution before (black lines) and after (red lines) wetting with secondary fluids: (a) octanol, (b) octanoic acid, (c) heptanoic acid, (d) heptane, (e) dodecane, and (f) toluene. The SFG spectra of the toluene-wetted samples were multiplied by 0.256.

widely used for fundamental studies of the interactions of nonadsorbing polymers with colloidal particles in water-based suspenions.[37,38] In the presence of PEO, the graphite system investigated here forms capillary suspensions with polar and nonpolar secondary fluids irrespective of the wetting angle. Vibrational SFG spectroscopy was employed to identify adsorbed species on the surface of graphite particles suspended in aqueous polymer solutions. Particles were deposited on glass substrates, and SFG spectra were recorded as described in sections 2.4 and 2.5. The corresponding results are shown in Figures 7 and 8. It should be noted that such experiments were not performed with PEO since first there is no indication that this polymer adsorbs to the graphite particles and second this polymer does not provide a characteristic resonance pattern in the frequency range accessible by the SFG technique. Particles suspended in CMC solution (black curves in Figure 7) exhibit a broad resonance pattern in the frequency range from 1300 to 1600 cm^{-1} with two maxima and a local minimum centered at ~1478 cm^{-1}. The shape of the SFG spectra in this frequency regime can be attributed to two vibrational bands with significant spectral overlap. The lower-frequency band at 1450 cm^{-1} originates from symmetric stretching vibrations of carboxylate ($R-COO^-$) groups at the interface[39] and is a clear signature of adsorbed CMC molecules. The second band at 1490 cm^{-1} is due to CH_2 scissoring vibrations from the carboxymethyl substituents. The observed frequency in the SFG spectra for symmetric carboxyl stretching vibrations is slightly shifted from the frequency of fully solvated carboxyl groups at around 1410 cm^{-1} [40] but is consistent with the frequency of carboxylates on ZnO nanoparticles in contact with air.[39] A close inspection of Figure 7 also reveals that the relative intensities of 1450 and 1490 cm^{-1} bands and their bandwidths varied between samples and caused weak but noticeable changes in the shape of the overall spectra. Presumably, these changes are caused by differences in the morphology of the particle layers, which may result in different wetting. However, the observed differences do not impair further analysis when the graphite particle layers are additionally covered by a secondary solvent in a subsequent step within one experimental run.

After the excess secondary solvent was removed, the particle layer was again analyzed using SFG spectroscopy; corresponding results are shown as red lines in Figure 7. Interestingly, the treatment with polar secondary fluids resulted in the complete disappearance of both vibrational bands at 1440 and 1490 cm^{-1} (red lines in Figure 7a,b), and SFG spectra were featureless with small nonresonant contributions. Similar spectra are obtained for clean graphite surfaces. Only when heptanoic acid was added were both bands still detectable, but with significantly reduced intensity (Figure 7c). From these observations, we conclude that secondary fluids with three-phase wetting angles of <90° wet the graphite surface and displace the adsorbed polymer molecules. Apparently, the addition of heptanoic acid does not result in the complete removal of CMC from the interfacial layer for the given experimental conditions.

The above-described experimental procedure was also performed using nonpolar secondary liquids, but in these cases, changes in the SFG spectra were negligible (Figure 7d–f). When dodecane and heptane were added, the SFG spectra remained unchanged as compared to the spectra of untreated samples (Figure 7d,e). The observed variation in spectral intensity is within experimental uncertainty. In the case of toluene, the overall pattern of the double-band feature shifted to higher frequencies and the intensity increased slightly (Figure 7f). This observation is interpreted as a structural

DOI: 10.1021/acs.langmuir.5b03861
Langmuir 2016, 32, 1440–1449

rearrangement of the adsorbed polymer molecules. However, even in this case the removal of CMC molecules from the particle surface can be excluded since the latter would lead to a decrease in SFG intensity and not to an increase.

Similar to the SFG experiments with CMC-covered graphite particles, we have recorded SFG spectra for particles that had a PVP adsorbate layer. Figure 8 shows SFG spectra of the latter prior to and after covering the particles with a secondary fluid and the subsequent removal of excess fluid. In the case of PVP, SFG spectra were dominated by a strong vibrational band at ~1695 cm^{-1} that is attributable to carbonyl (R−C═O) stretching vibrations of PVP adsorbates, while we attribute the much weaker and highly dispersive band at ~1490 cm^{-1} to CH_2 scissoring vibrations. A close inspection of Figure 8 reveals a similar trend for the displacement of PVP adsorbates due to the presence of a secondary fluid. While octanol, octanoic acid, and heptanoic acid lead to a complete loss of SFG intensity from PVP adsorbates which is indicative of a PVP displacement, SFG intensities of the PVP layer after covering the particles with heptane and dodecane remain unchanged. Different from the latter, the addition of toluene leads to an ~four-fold increase in SFG intensity (Figure 8f). Such an increase is consistent with the toluene-induced increase in the SFG signals of CMC adsorbates (Figure 7f) which we have attributed to a structural rearrangement of the CMC adsorbate layer. For PVP adsorbates, however, this rearrangement must be much more substantial. Taking the above results into account, we can conclude that in the case of PVP-covered graphite particles the secondary fluids with a three-phase wetting angle of $\Theta_{3p} < 90°$ also displace the PVP adsorbates, while the PVP layer remains surface-adsorbed in contact with secondary fluids for $\Theta_{3p} > 90°$.

Additional information was gained when the samples from SFG experiments were examined in an optical microscope using a combination of reflected and transmitted light. The untreated sample did show a random distribution of primary particles (Figure 9a). After the addition of the polar secondary liquids, a wetting film around the particles was found, and wetting layers located near particle agglomerates were observed even after thorough removal of the excess fluids (Figure 9b−d). The complete removal of secondary fluids was presumably suppressed by capillary forces present in the particle contact regions. No such residual wetting layers were observed after the addition and subsequent removal of excess fluid when nonpolar secondary liquids were used (Figure 9e−g).

From these investigations, we conclude that polar secondary fluids are able to replace adsorbed polymer molecules from graphite surfaces and can form pendular bridges, finally resulting in capillary suspensions with sample-spanning network structure. Nonpolar fluids do not interact with polymer-covered particles in a similar manner; CMC and PVP are not removed from the graphite surface and can thus provide steric repulsion strong enough to prevent the formation of stable particle clusters as building blocks for capillary-state capillary suspensions.[8] This seems to be in contradiction to the finding that the contact angle of nonwetting, nonpolar organic liquids does not vary with the adsorption of polymer (Figure 2). However, it has to be kept in mind that the range of steric repulsion is on the order of 50−100 nm according to the radius of gyration of the high-molecular-weight polymers used here.[41,42] However, the particles have to be in close contact in order to form stable clusters encapsulating small volumes of secondary liquid and serving as building blocks for the capillary-state network. Small changes in particle separation can result in an unstable cluster configuration at the high contact angle values relevant here.[8]

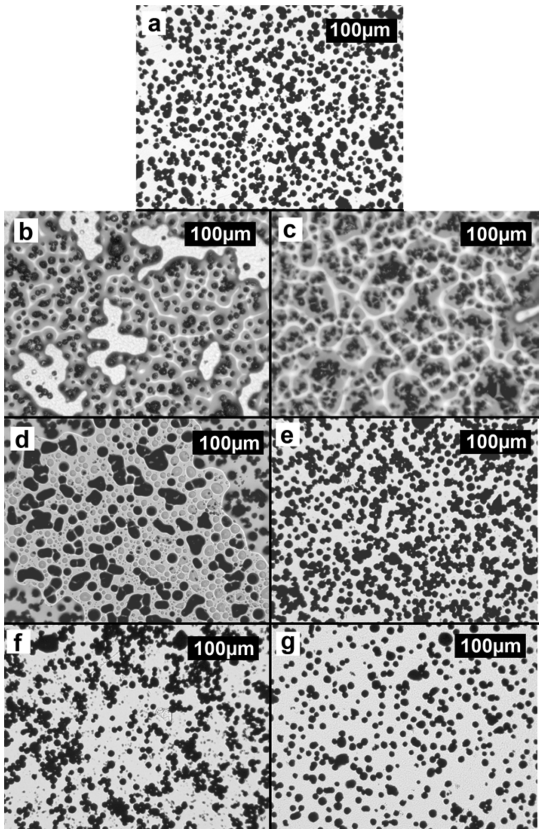

Figure 9. Optical microscopy images of graphite particles from CMC-based suspensions (a) before and after washing with (b) octanol, (c) octanoic acid, (d) heptanoic acid, (e) dodecane, (f) heptane, and (g) toluene.

4. SUMMARY AND CONCLUSIONS

Capillary suspensions are a novel formulation platform offering innovative solutions for creating materials with unique processing and end-use properties in various fields of application. Organic additives play a decisive role in many technical- and commercial-scale paste formulations. In this study, we used an aqueous suspension of non-Brownian graphite particles including adsorbing and nonadsorbing polymers in order to study the interaction between these ingredients and organic solvents added as secondary liquids and how this affects the characteristic structure formation in capillary suspensions.

Organic solvents with different polarity have been employed, and in the presence of the nonadsorbing PEO, all of them, whether they preferentially wet the graphite surface or not, induce the formation of a network structure within the suspension as indicated by the strong change in rheological properties. The low-shear viscosity increases by more than an order of magnitude, and a high, frequency-independent storage modulus emerges upon the addition of a secondary fluid.

However, when adsorbing polymers such as CMC and PVP are included, such structure formation and the drastic change in rheological behavior are observed only when polar organic solvents ($\Theta_{3p} < 90°$) are used as secondary liquids. Vibrational sum-frequency spectroscopy of the adsorbate layers provides evidence that these polar liquids remove the adsorbed polymer,

DOI: 10.1021/acs.langmuir.5b03861
Langmuir 2016, 32, 1440−1449

and they can form pendular bridges finally resulting in the formation of a sample-spanning particle network. In contrast, the nonpolar and nonwetting solvents do not force the desorption of the polymer from the particle surface. Moreover, the formation of particle clusters encapsulating the secondary liquid finally leading to gelation[8] does not take place, presumably due to the strong steric repulsion among graphite particles provided by the polymeric surface layers.

From these results, we conclude that polymeric additives and secondary fluids have to be carefully selected in suspension-based formulations when capillary forces are intended to be used for additional control of structure and flow behavior. Nevertheless, this offers a new pathway to customize paste formulations, the polymer may serve to adjust an appropriate viscosity level, and the capillary bridging induces the desired degree of shear thinning. Alternatively, the polymer may be selected with respect to its binding properties in the final dry product, and capillary bridging may be used to control the flow and processing behavior of the wet paste.

AUTHOR INFORMATION

Corresponding Author

*E-mail: boris.bitsch@kit.edu.

Notes

The authors declare no competing financial interest.

ACKNOWLEDGMENTS

B. Bitsch gratefully acknowledges financial support by the Heinrich Böll Foundation. Material donation by the Competence-E project (KIT) is appreciated. Special thanks go to P. Serpa, M. Frister, and O. Süß for experimental support. B. Braunschweig gratefully acknowledges support by Prof. W. Peukert (Friedrich-Alexander University Erlangen-Nürnberg).

REFERENCES

(1) Bröckel, U.; Meier, W.; Wagner, G. *Product Design and Engineering*; Wiley-VCH Verlag GmbH: Weinheim, Germany, 2013.

(2) Gompper, G.; Schick, M. *Soft Matter - Volume 2: Complex Colloidal Suspensions*; Wiley-VCH Verlag GmbH: Weinheim, Germany, 2005.

(3) Elias, H.-G. *An Introduction to Polymer Science (Chemistry)*; Wiley-VCH Verlag GmbH: Weinheim, Germany, 1997.

(4) Hiemenz, P. C.; Rajagopalan, R. *Principles of Colloid and Surface Chemistry, 3rd ed.*; CRC Press: New York, 1997.

(5) Koos, E.; Willenbacher, N. Capillary Forces in Suspension Rheology. *Science* **2011**, *331*, 897−900.

(6) Velankar, S. S. A Non-Equilibrium State Diagram for Liquid/fluid/particle Mixtures. *Soft Matter* **2015**, *11*, 8393−8403.

(7) Heidlebaugh, S. J.; Domenech, T.; Iasella, S. V.; Velankar, S. S. Aggregation and Separation in Ternary Particle/Oil/Water Systems with Fully Wettable Particles. *Langmuir* **2014**, *30* (1), 63−74.

(8) Koos, E.; Willenbacher, N. Particle Configurations and Gelation in Capillary Suspensions. *Soft Matter* **2012**, *8*, 3988−3994.

(9) Hoffmann, S.; Koos, E.; Willenbacher, N. Using Capillary Bridges to Tune Stability and Flow Behavior of Food Suspensions. *Food Hydrocolloids* **2014**, *40*, 44−52.

(10) Zhang, Y.; Allen, M. C.; Zhao, R.; Deheyn, D. D.; Behrens, S. H.; Meredith, J. C. Capillary Foams: Stabilization and Functionalization of Porous Liquids and Solids. *Langmuir* **2015**, *31* (9), 2669−2676.

(11) Zhang, Y.; Wu, J.; Wang, H.; Meredith, J. C.; Behrens, S. H. Stabilization of Liquid Foams through the Synergistic Action of Particles and an Immiscible Liquid. *Angew. Chem.* **2014**, *126*, 13603−13607.

(12) Bitsch, B.; Dittmann, J.; Schmitt, M.; Scharfer, P.; Schabel, W.; Willenbacher, N. A Novel Slurry Concept for the Fabrication of Lithium-Ion Battery Electrodes with Beneficial Properties. *J. Power Sources* **2014**, *265*, 81−90.

(13) Dittmann, J.; Koos, E.; Willenbacher, N. Ceramic Capillary Suspensions: Novel Processing Route for Macroporous Ceramic Materials. *J. Am. Ceram. Soc.* **2013**, *96* (2), 391−397.

(14) Maurath, J.; Dittmann, J.; Schultz, N.; Willenbacher, N. Fabrication of Highly Porous Glass Filters Using Capillary Suspension Processing. *Sep. Purif. Technol.* **2015**, *149*, 470−478.

(15) Domenech, T. E.; Velankar, S. S. Capillary-Driven Percolating Networks in Ternary Blends of Immiscible Polymers and Silica Particles. *Rheol. Acta* **2014**, *53*, 1−13.

(16) Xu, J.; Chen, L.; Choi, H.; Konish, H.; Li, X. Assembly of Metals and Nanoparticles into Novel Nanocomposite Superstructures. *Sci. Rep.* **2013**, *3*, 1730.

(17) Koos, E.; Johannsmeier, J.; Schwebler, L.; Willenbacher, N. Tuning Suspension Rheology Using Capillary Forces. *Soft Matter* **2012**, *8*, 6620−6628.

(18) Li, J.; Daniel, C.; Wood, D. Materials Processing for Lithium-Ion Batteries. *J. Power Sources* **2011**, *196* (5), 2452−2460.

(19) Xu, J. B.; Zhao, T. S. Mesoporous Carbon with Uniquely Combined Electrochemical and Mass Transport Characteristics for Polymer Electrolyte Membrane Fuel Cells. *RSC Adv.* **2013**, *3*, 16−24.

(20) Litster, S.; McLean, G. PEM Fuel Cell Electrodes. *J. Power Sources* **2004**, *130* (1−2), 61−76.

(21) Cheng, F.; Chen, J. Metal−air Batteries: From Oxygen Reduction Electrochemistry to Cathode Catalysts. *Chem. Soc. Rev.* **2012**, *41* (6), 2172−2192.

(22) Faraji, S.; Nasir, F. The Development Supercapacitor from Activated Carbon by Electroless Plating — A Review. *Renewable Sustainable Energy Rev.* **2015**, *42*, 823−834.

(23) Eissler, R. L.; Van Holde, K. E. *Wettability of Coal, Graphite, and Naphtalene As Measured by Contact Angles*; Circular 3; Department of Registration and Education: State of Illinois, 1962.

(24) Tsutsumi, K.; Ishida, S.; Shibata, K. Determination of the Surface Free Energy of Modified Carbon Fibers and Its Relation to the Work of Adhesion. *Colloid Polym. Sci.* **1990**, *268* (1), 31−37.

(25) Yang, H.; Yan, Y.; Zhu, P.; Li, H.; Zhu, Q.; Fan, C. Studies on the Viscosity Behavior of Polymer Solutions at Low Concentrations. *Eur. Polym. J.* **2005**, *41* (2), 329−340.

(26) Khan, M. S. Aggregate Formation in Poly(ethylene Oxide) Solutions. *J. Appl. Polym. Sci.* **2006**, *102* (3), 2578−2583.

(27) Richmond, G. L. Molecular Bonding and Interactions at Aqueous Surfaces as Probed by Vibrational Sum Frequency Spectroscopy. *Chem. Rev.* **2002**, *102* (8), 2693−2724.

(28) Shen, Y. R. *The Principles of Nonlinear Optics*; Wiley and Sons, 2002.

(29) Meltzer, C.; Dietrich, H.; Zahn, D.; Peukert, W.; Braunschweig, B. Self-Assembled Monolayers Get Their Final Finish via a Quasi-Langmuir−Blodgett Transfer. *Langmuir* **2015**, *31* (16), 4678−4685.

(30) Becker, R. S.; Freedman, K. A Comprehensive Investigation of the Mechanism and Photophysics of Isomerization of a Protonated and Unprotonated Schiff Base of 11-Cis-Retinal. *J. Am. Chem. Soc.* **1985**, *107* (6), 1477−1485.

(31) Cui, L.; Miao, X.; Xu, L.; Hu, Y.; Deng, W. Self-Assembly Polymorphism of 2,7-Bis-Nonyloxy- 9-Fluorenone: Solvent Induced the Diversity of Intermolecular Dipole−dipole Interactions. *Phys. Chem. Chem. Phys.* **2015**, *17*, 3627−3636.

(32) Esumi, K.; Ishizuki, K.; Otsuka, H.; Ono, M.; Ichikawa, S.; Yanase, C. The Effect of Binary Solvents on Adsorption of Poly(vinylpyrrolidone) on Titanium Dioxide and Graphite Particles. *J. Colloid Interface Sci.* **1996**, *178* (2), 549−554.

(33) Lee, J.-H.; Paik, U.; Hackley, V. a.; Choi, Y.-M. Effect of Carboxymethyl Cellulose on Aqueous Processing of Natural Graphite Negative Electrodes and Their Electrochemical Performance for Lithium Batteries. *J. Electrochem. Soc.* **2005**, *152* (9), A1763−A1769.

(34) Solaris, J. a.; Araujo, a. C. De; Laskowski, J. S. The Effect of Carboxymethyl Cellulose on the Flotation and Surface Properties of Graphite. *Coal Prep.* **1986**, *3* (1), 15−31.

DOI: 10.1021/acs.langmuir.5b03861
Langmuir 2016, 32, 1440−1449

(35) Krieger, I. M.; Dougherty, T. J. A Mechanism for Non-Newtonian Flow in Suspensions of Rigid Spheres. *J. Rheol.* **1959**, *3* (1), 137−152.
(36) Quemada, D. Rheology of Concentrated Disperse Systems and Minimum Energy Dissipation. *Rheol. Acta* **1977**, *16*, 82−94.
(37) Olsson, M.; Joabsson, F.; Piculell, L. Particle-Induced Phase Separation in Mixed Polymer Solutions. *Langmuir* **2005**, *21* (5), 1560−1567.
(38) McFarlane, N. L.; Wagner, N. J.; Kaler, E. W.; Lynch, M. L. Poly(ethylene Oxide) (PEO) and Poly(vinyl Pyrolidone) (PVP) Induce Different Changes in the Colloid Stability of Nanoparticles. *Langmuir* **2010**, *26* (17), 13823−13830.
(39) Faber, H.; Hirschmann, J.; Klaumünzer, M.; Braunschweig, B.; Peukert, W.; Halik, M. Impact of Oxygen Plasma Treatment on the Device Performance of Zinc Oxide Nanoparticle-Based Thin-Film Transistors. *ACS Appl. Mater. Interfaces* **2012**, *4* (3), 1693−1696.
(40) Cuba-Chiem, L. T.; Huynh, L.; Ralston, J.; Beattie, D. a. In Situ Particle Film ATR FTIR Spectroscopy of Carboxymethyl Cellulose Adsorption on Talc: Binding Mechanism, pH Effects, and Adsorption Kinetics. *Langmuir* **2008**, *24* (15), 8036−8044.
(41) Hoogendam, C.; Peters, J.; Tuinier, R.; de Keizer, A.; Cohen Stuart, M. A.; Bijsterbosch, B. Effective Viscosity of Polymer Solutions: Relation to the Determination of the Depletion Thickness and Thickness of the Adsorbed Layer of Cellulose Derivatives. *J. Colloid Interface Sci.* **1998**, *207*, 309−316.
(42) Matsudo, T.; Ogawa, K.; Kokufuta, E. Complex Formation of Protein with Different Water-Soluble Synthetic Polymers. *Biomacromolecules* **2003**, *4*, 1794−1799.

DOI: 10.1021/acs.langmuir.5b03861
Langmuir 2016, 32, 1440−1449